# Hygroexpansion, Surface Roughness and Porosity Affect the Electrical Resistance of EVOH-Aluminum-Coated Paper

**Martina Lindner** [1,2,]*[ID]**, Matthias Reinelt** [2]**, Tobias Gilch** [2,3] **and Horst-Christian Langowski** [1,2]

[1]  TUM School of Life Sciences Weihenstephan, Technical University of Munich, Weihenstephaner Steig 22, 85354 Freising, Germany; horst-christian.langowski@ivv.fraunhofer.de
[2]  Fraunhofer-Institute for Process Engineering and Packaging IVV, Giggenhauser Strasse 35, 85354 Freising, Germany; matthias.reinelt@ivv.fraunhofer.de (M.R.); tobias.gilch@ivv.fraunhofer.de (T.G.)
[3]  Munich University of Applied Sciences, Lothstraße 35, 80335 Munich, Germany
\*  Correspondence: martina.lindner@ivv.fraunhofer.de; Tel.: +49-8161-491-536

check for updates

**Abstract:** When aluminum is applied to paper by physical vapor deposition, substrate roughness contributes to the defect density and hygroexpansion can cause defects that impair the aluminum coating. Both effects can manifest as an increase in electrical resistance. We quantified the effect of substrate paper hygroexpansion (0–95% relative humidity) and paper surface roughness on the effective resistivity ($\rho_{EFF}$) of aluminum coatings. To create different degrees of roughness, five different papers were used. Each of them had one pigment coated side and one side without pigment coating. These different rough paper surfaces were pre-coated with ethylene vinyl alcohol co-polymer (EVOH). Hygroexpansion was promoted by pre-coating and increased more when the coating was applied on rough and porous surfaces. Simultaneously, the pre-coating reduced surface roughness; especially porosity. The reduction of porosity decreased effective resistivity ($\rho_{EFF}$). Based on these results, an aluminum thickness of ≥35 nm is recommended to ensure maximum mechanical stability during hygroexpansion in combination with minimum material usage. Moreover, the resistivity did not regain its initial value when the paper substrate shrank during re-drying.

**Keywords:** resistivity; physical vapor deposition; sheet resistance; ethylene vinyl alcohol; paper coating; penetration; porosity; sorption; humidity

## 1. Introduction

When nanometer thin coatings of aluminum are deposited on paper substrates, the substrate roughness determines its electrical resistance; and hygroexpansion manifests as an increase in electrical resistance and resistivity (compared to bulk aluminum) [1]. These phenomena reflect the greater number of defects in the aluminum layer. Defects triggered by hygroexpansion and roughness are relevant in various applications, such as packaging, paper electronics and flexible electronics.

In the case of packaging, aluminum coatings are used to create high gas barriers on polymer substrates. However, it is not yet possible, to achieve such gas barriers on paper substrates, because the aluminum coatings contain defects, which let gas permeate. In the case of paper electronics, such defects increase the resistance of the aluminum conductor coating. Although in the case of packaging applications, the effect of aluminum defects is a higher gas permeability, in both cases—packaging and paper electronics—defects can manifest as an increase in electrical resistance and resistivity. Two known reasons for such defects are substrate hygroexpansion and substrate roughness [1,2]. Hygroexpansion is the moisture-induced swelling of paper. Hygroexpansion and paper roughness can be altered by various methods during [3–10] or after [11–14] paper production. In the present case, the effect of

a polymer coating on both parameters—roughness and hygroexpansion—was evaluated. Previous studies [1,2] have shown that the effective resistivity $\rho_{EFF}$ (defined by the measured resistance, coating weight of aluminum and ideal density; compare Equations (2)–(4) of such thin aluminum layers is not constant but decreases with increasing thickness ($d$) and decreasing substrate roughness ($R_Z$) [15,16]. The correlation can be described using Equation (1), which includes two fit factors ($k$ and $c$) and the literature resistance value for bulk aluminum ($\rho_{lit}$) [1].

$$\rho_{EFF} = R_Z \cdot c \cdot \frac{1}{d} + \rho_{lit} \cdot (1 + R_Z \cdot k)$$

$$\rho_{lit} = 27 \ \Omega \cdot nm \quad k = 0.5/\mu m \quad c = 2964 \ \Omega \cdot nm^2/\mu m$$

(1)

Even though the relationship between roughness and resistivity can be well described, as in Equation (1), this is not yet the case for hygroexpansion and resistivity. The effect of hygroexpansion on electrical resistivity is much more complex, because the effect of hygroexpansion itself is also affected by the substrate roughness. As both processes are relevant for packaging and paper electronic applications, the current study investigates in depth the effect of substrate roughness on the increase in electrical resistivity during hygroexpansion. Different degrees of roughness were created by using different substrate papers with different rough back and front surfaces, either with a pigment coating (PC) or without (noPC), and by pre-coating the surfaces with ethylene vinyl alcohol co-polymer (EVOH) before aluminum deposition. The electrical resistivity of the aluminum coatings was then determined at different levels of relative humidity (*RH*). The aluminum thickness was varied to define the influence of this parameter.

## 2. Materials and Methods

### 2.1. Used Papers

The paper substrates were chosen as they are typically applied for metallization processes in the packaging industry. They are listed in Table 1. Each of the papers had one side, which is pigment coated (PC) and one side, which has not been pigment coated (noPC).

**Table 1.** Paper and polymer substrates.

| Product Name | Grammage [g/m$^2$] | Supplier |
|---|---|---|
| Metalkote | 65 | Ahlstrom-Munksjö |
| Algro Finesse T | 70 | Sappi Europe SA |
| Adicar WS HGM | 80 | Cham Paper Group |
| Adicar 2 | 80 | Cham Paper Group |
| Labelcar MTS | 65 | Cham Paper Group |

### 2.2. Preparation of Aqueous EVOH Solutions

EVOH is known to be a water sensitive polymer and is often used to reduce the oxygen permeability of coated papers [17]. The required amount (15% *w/w*) of EVOH granulate (AQ4104, Kuraray, Frankfurt am Main, Germany) was mixed with the required amount of deionized water in a high-performance disperser (Thermomix TM 31, Vorwerk Deutschland, Wuppertal, Germany) at low stirring speed (40 rpm) for 15 min. Then, the disperser was set to 100 rpm for 90 min, heating up continually to 90 °C. Afterward the solution was stirred at 40 rpm for 120 min, while cooling to room temperature. The solution was then filtered and filled into a glass bottle, which was sonicated at 37 kHz and 10 °C for 10 min to remove air bubbles. The ethylene content of this EVOH grade was ~8 mol% [18].

### 2.3. Laboratory-Scale EVOH Coating

The paper types Adicar 2, Adicar WS HGM, Algro Finesse T and Labelcar MTS were only available as sheets, and were, therefore, coated using laboratory-scale equipment (CUF 5, Sumet Systems GmbH,

Denklingen, Germany). Each paper was coated once on PC and once on noPC (Figure 1). The substrate sheet was fixed with a clamp on a horizontal slide and a wired rod—with a theoretical wet coating thickness of 19 μm—was positioned on the top of the sheet and forced onto the sheet by applying a force of 40 N. Approximately 5 mL of the EVOH solution was applied with a syringe into the gap between the rod and the substrate across the width of the sheet. The slide was then moved horizontally below the rod (40 mm/s) to ensure even distribution across the paper sheet. The slide was then passed through a drying section to dry the coated paper by air convection at 85 °C for 90 s.
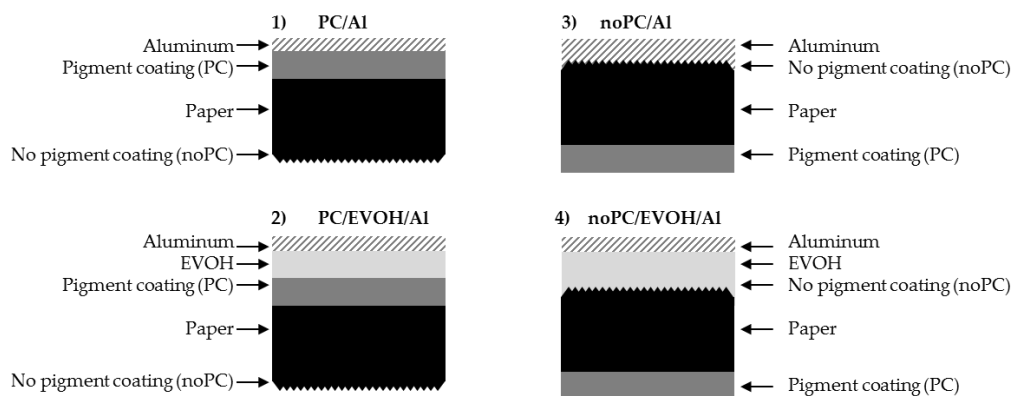


**Figure 1.** A schematic description of the samples that were produced, as described in the previous enumeration.

## 2.4. Pilot-Scale EVOH Coating

Metalkote paper was coated in a reel-to-reel process using the lacquering and lamination plant at Fraunhofer IVV. It was coated once on PC and once on noPC. The coating width was 210 mm at a web speed of 5 m/min, with an anilox ceramic roll (40 lines/cm, 45° pattern, theoretical pick-up volume 45 mL/m$^2$) and a convective air drying temperature of 85 °C, with an air flow rate of 8000 m$^3$/h.

## 2.5. EVOH Coating Weight Determination

Samples were stored at 23 °C, 50% *RH* for 48 h. Then, five circles with an area of 50 cm$^2$ were cut from the EVOH-coated and non-coated papers. Subsequently, the weight of the samples was determined (Mettler AT261 DeltaRange, Mettler-Toledo, Gießen, Germany). The coating weight was determined as the weight difference between EVOH-coated and non-coated papers, normalized to an area of 1 m$^2$.

## 2.6. Physical Vapor Deposited (PVD) Aluminum Coating

The following samples were produced by PVD coating (Figure 1).

1. PC/Al: Aluminum was deposited on the paper side, that has been pigment coated;
2. PC/EVOH/Al: The paper was first coated with EVOH on the paper side, that has been pigment coated, and then aluminum was deposited on top of the EVOH;
3. noPC/Al: Aluminum was deposited on the paper side, which has not been pigment coated;
4. noPC/EVOH/Al: The paper was first coated with EVOH on the paper side, that has not been clay coated, then aluminum deposited was on top of the EVOH.

Paper samples were cut to 105 × 148 mm$^2$ sheets and taped along all four edges onto a paper carrier roll using thermally stable adhesive tape (Kapton, DuPont, Neu-Isenburg, Germany). In order to achieve a high vacuum during PVD, it was necessary to reduce the moisture content (*mc*) of the paper substrate. Therefore, the carrier roll containing all the samples was dried at 70 °C for 9 days in a Heratherm oven (Thermo Fisher Scientific, Munich, Germany) prior to metallization, which is not an industrial process but necessary in pilot plant scale.

PVD was carried out using the electron beam heating method. Moisture remaining in the chamber was extracted using a Meissner cold trap and the deposition roll was water cooled. The aluminum was 99.98% pure (K135 from Drahtwerk Elisental W. Erdmann GmbH & Co., Neuenrade, Germany). The coating thickness was varied by changing the web speed from 0.5 to 3.5 m/min at steps of 0.5 m/min at an evaporation rate of 2–3.5 nm/s. Further process details can be found elsewhere [19].

Following their removal from the box coater, the rolls were transferred to an polyethylene drum containing 1 kg Perlform silica gel (orange, 2–5 mm, with an indicator; Carl Roth, Karlsruhe, Germany) to reduce the *RH* to 0%. As such, the unwanted water uptake and hygroexpansion of the paper before the experiments was kept to a minimum. The drum was then stored at 23 °C.

## 2.7. Aluminum Coating Weight Determination

The coating weight ($cw_{NOMINAL}$) and thickness ($d_{NOMINAL}$) of aluminum applied to the surface of each sample was calculated based on a previously described model [19]. Both values are linked by the literature value for aluminum density ($\delta_{LIT}$) as shown in Equation (2).

$$cw_{NOMINAL} = d_{NOMINAL} \cdot \delta_{LIT}. \tag{2}$$

## 2.8. Scanning Electron Microscopy (SEM)

Images were acquired using a JSM-7200F scanning electron microscope (Jeol, Peabody, MA, USA) at 1–4 kV. The working distance was maintained at 9.1–10.0 mm. The samples were sputtered with gold.

## 2.9. Determination of Sheet Resistance via Eddy Currents at Different Relative Humdities

Prior to re-humidification of the aluminum-coated samples, rigid frames were produced to which the samples were loosely attached to avoid curling. In the next step, the plastic frames, the silica pouches, a dish containing 500 g silica gel, a pair of scissors, pressure lock bags, adhesive tape, a testostor 175 hygrometer (Testo SE & Co. KGaA, Lenzkirch, Germany), and Fibox oxygen concentration measuring points (PreSens Precision Sensing, Regensburg, Germany) were placed into a glove box (Mecaplex Metall, Grenchen, Switzerland). Finally, the roll with the aluminum-coated samples was placed into the glove box, which was immediately closed and flushed with pure nitrogen to remove moisture. Flushing was assumed to be complete when a constant, minimal *RH* value of <3% (determined using the hygrometer) was reached. The paper samples were then removed from the carrier roll and attached to the frames with adhesive tape. The samples were transferred into the pressure lock bags. After transferring all samples into these bags, the glove box was opened and the pressure lock bags were placed in the plastic drum with fresh silica gel.

The samples were then taken one by one from the drum and the sheet resistance was measured at five predetermined points on each sample. After this first measurement at 0% *RH*, the samples were immediately transferred to a KBF720-230V climate chamber (Binder, Tuttlingen, Germany) set to 23 °C, with humidity values of 35%, 50%, 70%, 85% and 95% *RH*. The samples were stored in each climate for 24 h before the next measurement of sheet resistance. After each measurement, the samples were placed back into the climate chamber. Excessive air convection in the chamber was avoided by using additional plastic curtains placed inside the chamber.

The sheet resistance ($R_{\blacksquare}$) was measured using the eddy current method (EddyCus TF lab 4040, Suragus, Dresden, Germany). The skin depth was >8 μm [20,21], which ensured full penetration of the aluminum layer by the magnetic field. The area captured by the measurement was approximately 5 × 5 mm$^2$. The sheet resistance ($R_{\blacksquare}$) of a resistor with thickness $d$ and resistivity $\rho$ is defined as shown in Equation (3).

$$R_{\blacksquare} = \frac{\rho}{d} \tag{3}$$

The effective resistivity ($\rho_{EFF}$) was then calculated from the thickness ($d_{NOMINAL}$) and the measured sheet resistance ($R_{\blacksquare}$) as shown in Equation (4).

$$\rho_{EFF} = d_{NOMINAL} \cdot R_{\blacksquare} \tag{4}$$

The relative effective resistivity increase ($\gamma$) was calculated from the effective resistivity at an *RH* of 0% and at a given *RH* of $x$%, where $x$ = 35%, 50%, 70%, 85% or 95% *RH*, as shown in Equation (5).

$$\gamma = \frac{\rho_{EFF}^{RH=x}}{\rho_{EFF}^{RH=0\%}} - 1 \tag{5}$$

The theoretical increase in resistivity $\gamma$ due to the mono-axial expansion of aluminum without any damaging effect can be estimated by the following assumption: The volume of aluminum (cross-section $A \times$ length $L$) is constant under strain $\varepsilon$, namely $A \cdot L = A_0 \cdot L_0$. Under strain, the material expands in length but also thins. Thus, $A$ decreases and $L$ increases due to plastic deformation. Based on that assumption, Equations (6)–(8) can be derived [22].

$$\frac{R_{\blacksquare}}{R_{\blacksquare 0}} = \left(\frac{L}{L_0}\right)^2 \tag{6}$$

$$\frac{\rho_{EFF}}{\rho_{EFF,0}} = \left(\frac{L}{L_0}\right)^2 = (1+\varepsilon)^2 \tag{7}$$

$$\gamma = \frac{\rho_{EFF}}{\rho_{EFF,0}} - 1 = (1+\varepsilon)^2 - 1 \tag{8}$$

## 2.10. Sorption Isotherm

Sorption isotherms for the paper substrates were recorded at 0%, 35%, 50%, 70%, 85% and 95% *RH* using SPSx-1µ (ProUmid GmbH & Co. KG, Ulm, Germany). The temperature was set to 23 °C. For each humidity increase, the weight was measured until equilibrium was reached. The minimum time for each *RH* increase was set to 2 h, and the maximum to 48 h. The measurements were done once on the pure papers and twice on the EVOH-coated papers.

## 2.11. Hygroexpansion

The hygroexpansion measurement was carried out on three samples ($288 \times 200$ mm$^2$) from each paper. The samples were dried for 20 days in silica gel at 23 °C. Then, each was stored in the KBF720-230V climate chamber (Binder, Tuttlingen, Germany) at 23 °C for 24 h, with sequentially increasing humidity values of 35%, 50%, 70%, 85% and 95% *RH*. The samples were taken one by one from the drum/climate chamber and their size was scanned at a resolution of 1200 dpi (CanonScan LiDE 700F, Canon, Nürnberg, Germany). Images were saved as jpg files. Subsequently, the distance ($L_{0,CD}$) between certain reference points in CD (cross direction) was measured threefold, using LAS v4.0 software (Leica Microsystems GmbH). Measurements were only performed in CD because hygroexpansion is dominant in this direction. From these data, the percentage length increase $\varepsilon$ at increasing *RH* values was calculated by setting $L_{0,CD}$ in relation to the increased lengths $L_{CD}$ as shown in Equation (9).

$$\varepsilon_{CD} = \frac{L_{CD} - L_{0,CD}}{L_{0,CD}} \tag{9}$$

## 2.12. Surface Roughness

The roughness was determined five-fold using the mechanical profile method (Hommel Etamic W55, Jenoptik, Jena, Germany). The roughness term $R_Z$ was taken according to DIN EN ISO

4288:1998 [16] and DIN EN ISO 3274:1998 [15]: The traversing length $L_N$ is divided into five equal-sized subsections $L_R$ (in this case, $L_N = 4$ and $L_N = 12.5$, respectively). In the single subsections, the single roughness ($Z_N$) was determined. The single roughness is the difference between the highest and lowest points in one subsection $L_R$ [23]. From $Z_N$, $R_Z$ is determined as their arithmetic average. The value $R_Z$ was used, as the graphs do not significantly change when other roughness values such as $R_a$ and $R_q$ are used. The usage of $R_{Pc}$ was evaluated but was found to lead to inconsistent results because of the necessary adaption of the counting threshold.

## 2.13. Statistical Methods

The data points represent median values for resistances and average values for roughness. The statistical differences were evaluated with a u-test from Wilcoxon, Mann and Whitney, with the level considered significant when equal to 5%. Graphs were designed using OriginPro 2016 (version 2018.b) and statistical evaluations were carried out with Visual-XSel (CRGRAPH) (version 12.0).

## 3. Results and Discussion

### 3.1. Effect of Polymer Coatings on Paper Hygroexpansion

In the first set of experiments, we determined the effect of EVOH coatings on paper hygroexpansion and water absorption using five different papers, which were EVOH coated either on the side with pigment or without pigment coating (PC vs noPC). Initially, we measured the coating weight. Although in each case the same EVOH coating and the same rod was used, the coating weight of the EVOH coating was higher on noPC paper (Figure 2). This reflected the fact that noPC paper is rougher and more porous, so the EVOH could penetrate into the paper more easily (Figure 3) [24–27]. However, the coating weight did not show a linear correlation with roughness ($R_Z$), probably because the roughness value does not sufficiently describe the porosity of the paper sample.
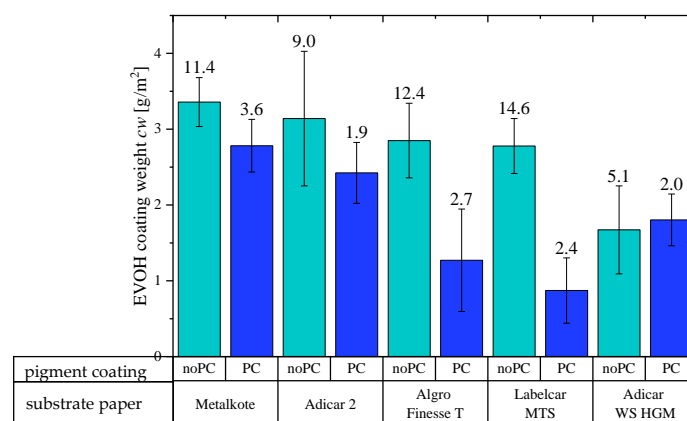


**Figure 2.** Coating weight at 50% relative humidity. Although in each case the same EVOH coating and the same rod was used, the weight of the EVOH coating was higher on the rougher noPC surface. Roughness values $R_Z$ before EVOH coating are shown as numbers above the columns. PC/noPC = paper surface with/without pigment coating. EVOH = ethylene vinyl alcohol lacquer.
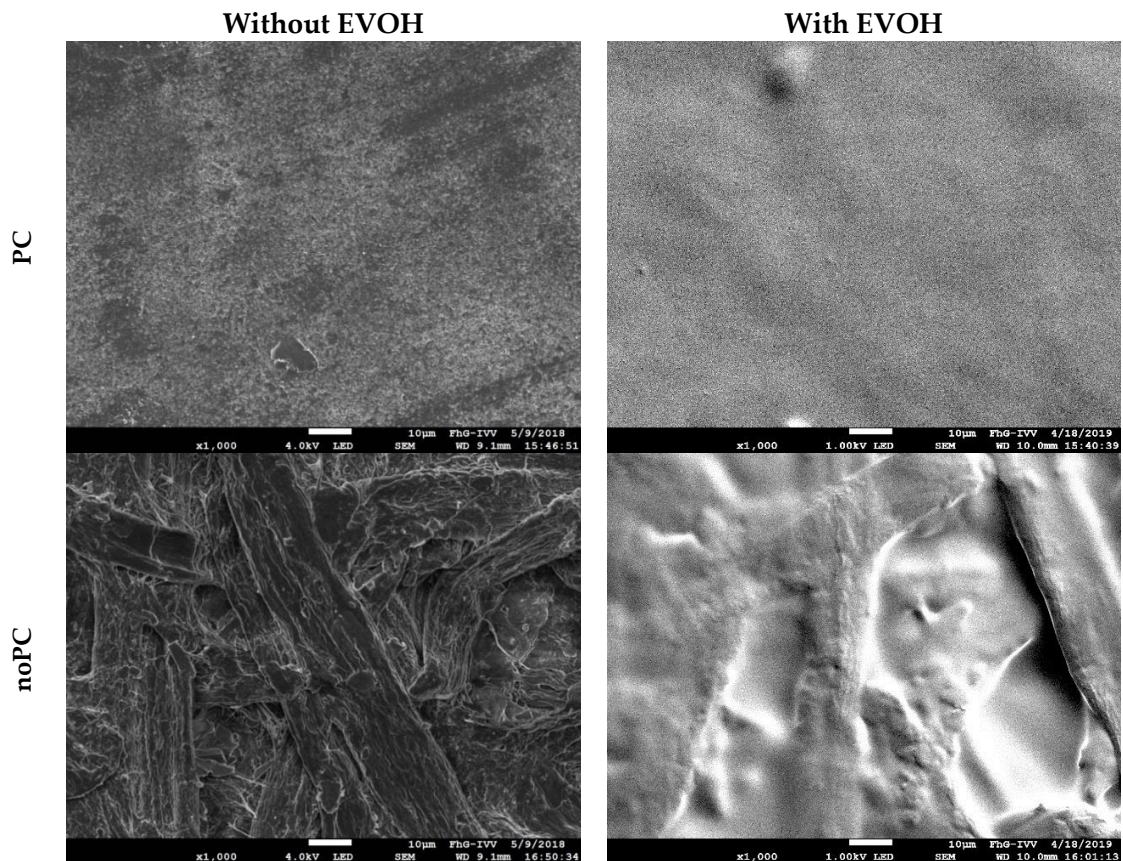
**Figure 3.** Scanning electron microscope images at 1000 times magnification of Metalkote paper. The EVOH-coated paper shows lower roughness and lower porosity.

Next, we measured the moisture sorption and hygroexpansion of the coated and non-coated papers. We found that EVOH increased the water absorption (Figure 4, left column) compared to the pure paper (–■–) but the absorption was the same regardless of the side of the paper to which the EVOH was applied (PC –▼– or noPC –●–). This reflected the relatively low coating weight (~1–3 g/m$^2$) compared to the paper grammage (65–80 g/m$^2$). In contrast, hygroexpansion (Figure 4, right column) was strongly affected by the side to which the EVOH was applied. The effect was not visible in the case of Adicar WSHGM, as the differences in roughness and coating weight between noPC and PC was low. The hygroexpansion was higher for the EVOH-coated papers than for the pure paper, but highest when EVOH was applied to the noPC side (–●–). This indicated that the EVOH penetrated further into the noPC side of the paper because the surface contained more pores and channels (see images presented in [1]). EVOH thus fills the voids in the noPC paper and occupies space that the fibers would otherwise fill during expansion. This interpretation is supported by reference [28]. Because this space between the fibers is now occupied by EVOH, the paper expands further, particularly on the noPC side where more EVOH has penetrated between the fibers. This is because EVOH does not prevent water molecules from permeating towards the fibers, but it allows water molecules to permeate towards the fibers, which leads to fiber hygroexpansion. Moreover, the EVOH itself absorbs water and swells, which further intensifies the effect (lacquer hygroexpansion of ~5% and moisture content of 30% at 100% *RH* at 23 °C).
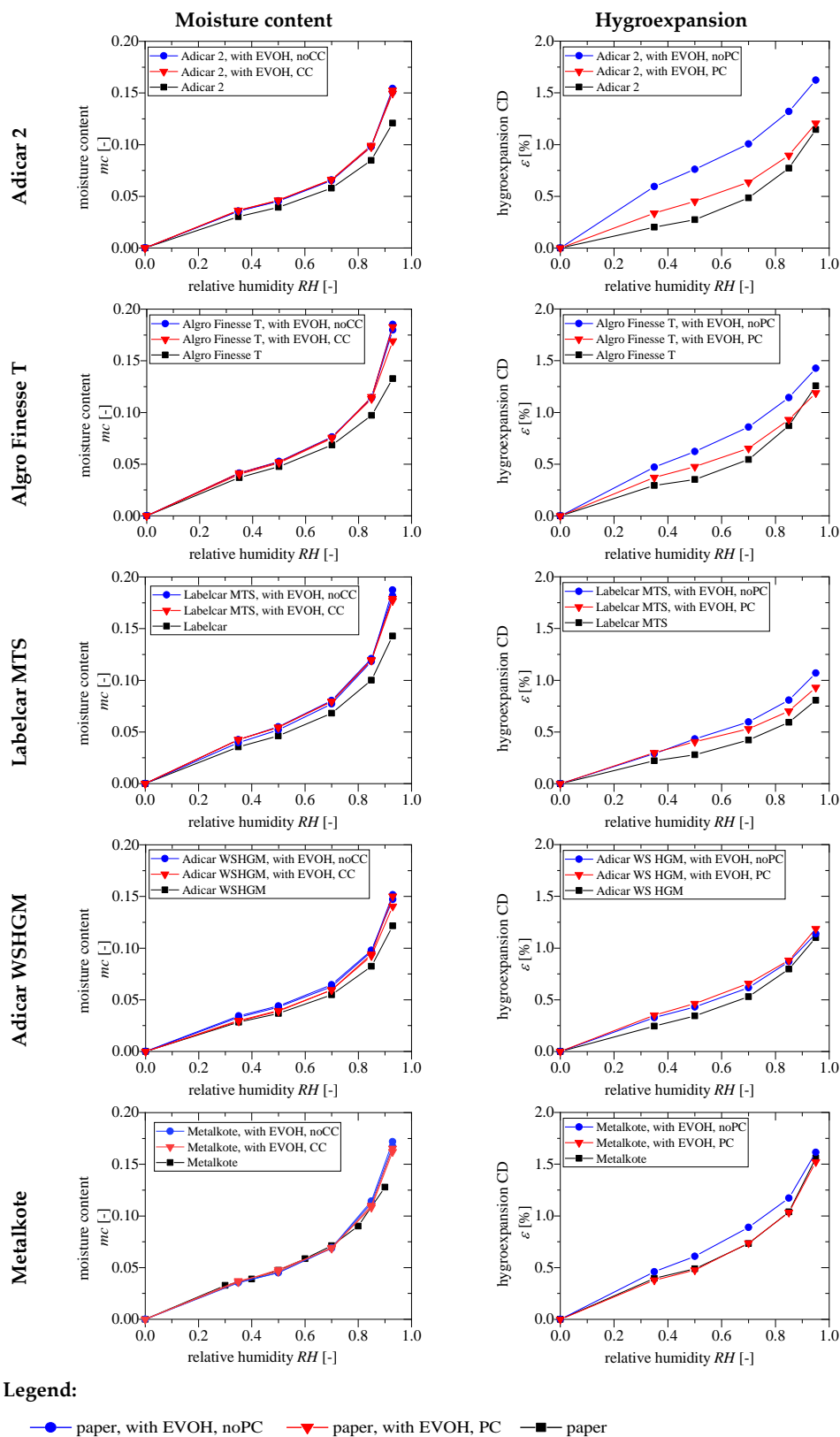
**Figure 4.** Moisture content (*mc*) and hygroexpansion (*ε*) increase with relative humidity (*RH*). The EVOH coating increased moisture content and hygroexpansion. Hygroexpansion increased more when the EVOH was applied to the noPC surface. PC/noPC = paper surface with/without pigment coating. EVOH = ethylene vinyl alcohol lacquer.

### 3.2. Effect of EVOH Pre-coating on Effective Resistivity of the Aluminum Coating

As we previously reported in reference [1], the effective resistivity $\rho_{EFF}$ decreased with aluminum thickness and increased with substrate roughness, which was also confirmed in Figure 5. There, we found that curves—as in Figure 5—showed a characteristic minimum resistivity value $\rho_{OFFSET}$ [Ω·nm] when the aluminum layer was thickest, overlaid by a variable resistivity $\rho_n$ [Ω·nm] when the layer was thinner. Even for the thicker coatings, the minimum resistivity $\rho_{OFFSET}$ would not achieve the literature values for bulk aluminum $\rho_{lit}$. In the same previous study [1], this minimum resistivity $\rho_{OFFSET}$ decreased with decreasing substrate roughness, possibly because less roughness led to smaller defects, which were easily filled with aluminum. In comparison, defects on very rough papers were too large to be filled, thus increasing the resistance $R$ and minimum resistivity $\rho_{OFFSET}$. For thin coatings, the resistivity was higher on rough substrates, and the variable resistivity $\rho_n$, therefore, also depended on paper roughness $R_Z$. Moreover, thinner coatings led to higher variable resistivity $\rho_n$ because less aluminum was available to fill the defects. These observations have been combined with the simple descriptive approach shown in Equation (1).
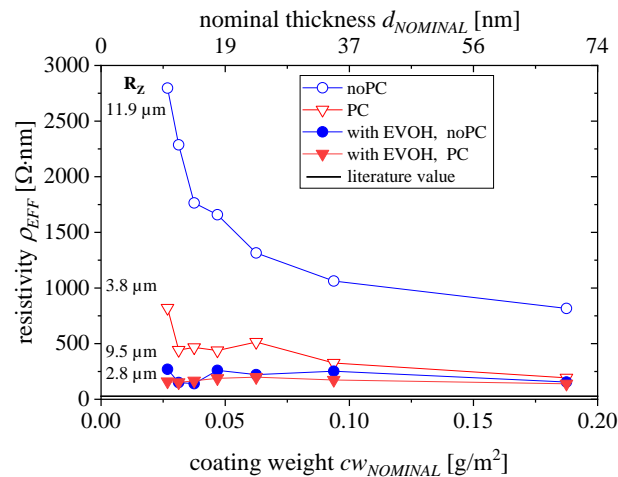


**Figure 5.** Increasing roughness increased the effective resistivity at 0% relative humidity (*RH*) due to defects in the aluminum coating. Although EVOH coating only had a minor impact on roughness ($R_Z$) values, the resistivity decreased massively due to the reduction of the areal density of micropores and channels. Results were generated on Metalkote paper. PC/noPC = paper surface with/without pigment coating. EVOH = ethylene vinyl alcohol lacquer.

However, the present study shows that substrate roughness cannot be the only influencing factor and the following conclusions can be drawn from Figure 5:

1.  The resistivity of aluminum applied to EVOH-coated surfaces was lower than on surfaces without EVOH. This supports the observation described previously [1];
2.  However, the roughness of noPC with EVOH (—•—, $R_Z$ = 9.5 μm) was much higher than PC (—▽— $R_Z$ = 3.8 μm). Nevertheless, noPC with EVOH (—•—) had a lower resistivity than PC (—▽—);
3.  This indicates that, not only the roughness, but also the precise morphology—including pores and microchannels—were decisive factors. EVOH coatings may fill up pores and microchannels, but they did not affect the micrometer-scale roughness significantly (compare Figure 3);
4.  This filling up of voids facilitated the formation of a closed aluminum layer because it reduced the severity of defects in the aluminum coating. As shown in Section 3.1, the filling up of voids promoted hygroexpansion and EVOH should, therefore, be applied on the PC side of the paper.

### 3.3. Effect of EVOH Pre-Coating on the Increase in Resistivity during Hygroexpansion

It is likely that the aluminum coating forms cracks when the underlying paper expands, thus increasing the resistivity, and that greater substrate roughness leads to more cracks and thus to a higher increase in effective resistivity ($\gamma$). In order to show the effect of hygroexpansion and roughness in isolation from the effect of aluminum thickness, the relative effective resistivity increase $\gamma$ (rather than resistance $R_\blacksquare$ or effective resistivity $\rho_{EFF}$) was considered, as shown in Figure 6.
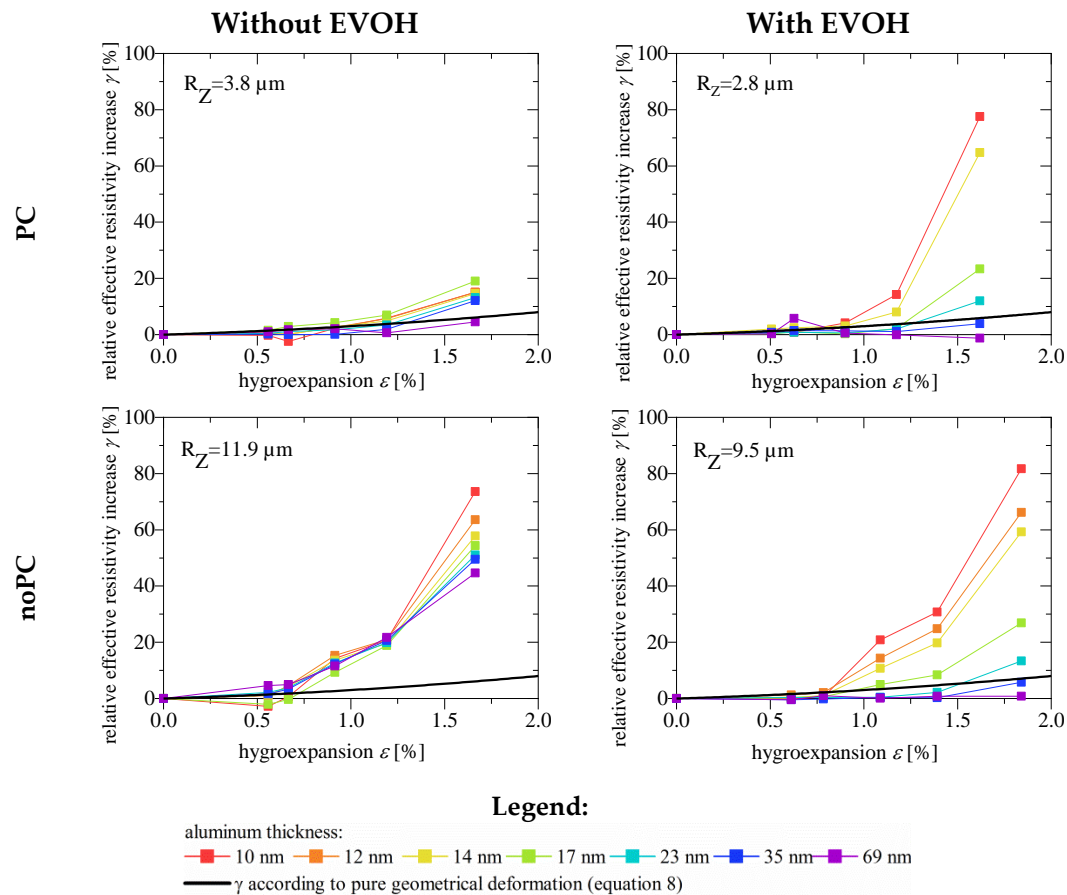


**Figure 6.** Increasing roughness $R_Z$ and porosity of the substrate paper Metalkote increased the effective resistivity $\rho_{EFF}$ due to defects in the aluminum coating. Although the EVOH coating only had a minor impact on roughness values $R_Z$, the resistivity was lower due to the lower porosity. PC/noPC = paper surface with/without pigment coating. EVOH = ethylene vinyl alcohol lacquer.

We found that the difference between the EVOH-coated and non-coated surfaces subsequently affects the relative effective resistivity increase $\gamma$ during hygroexpansion. The increase in resistivity for PC and noPC paper surfaces with and without EVOH, and with aluminum layers differing in thicknesses, is summarized in Figure 6. The comparison of the different samples allows the following conclusions to be drawn:

1. The relative effective resistivity increase $\gamma$ correlated with hygroexpansion $\varepsilon$;
2. The maximum relative effective resistivity increase $\gamma_{max}$ at 95% *RH* was partially higher on EVOH-coated surfaces (Figure 6). This was because the initial effective resistivity values $\rho_{EFF}$ (Figure 5) were much lower; probably due to fewer initial defects. Therefore, the addition of only a few more defects increased the resistivity by a much greater degree. This means that $\gamma_{max}$ also depended on the initial $\rho_{EFF}$ before hygroexpansion, which was higher on rough and porous surfaces;

3.  In the ideal case (smooth substrate surface, low hygroexpansion, and thick coatings) $\gamma$ was equal to the value expected, according to the geometrical deformation model in Equation (8). This indicated that no additional defects occurred during hygroexpansion and that no additional defects should be expected in the case of smooth substrates and thick coatings (>35 nm);

4.  On EVOH-coated surfaces, the effect of the aluminum thickness (*d*) was more explicit. Thinner coatings (<35 nm) led to a higher relative effective resistivity increase $\gamma$. Coatings >35 nm are, therefore, recommended;

5.  On surfaces without EVOH, the effect of the aluminum thickness was less explicit. On non-EVOH coated surfaces, the effect of aluminum thickness on the increase in $\gamma$ was lower because the aluminum already contained many defects before hygroexpansion, due to its roughness and porosity (Figure 3). Hence the additional defects due to hygroexpansion did not significantly affect the resistivity value. The EVOH decreased the roughness ($R_Z$) and the areal density of pores and microchannels. For practical applications, this means that even by applying thicker aluminum coatings, the negative effect of roughness and pores during hygroexpansion cannot be reduced. Thus, a polymer pre-coating such as EVOH is indispensable;

6.  The effect of aluminum thickness on the maximum relative effective resistivity increase $\gamma_{max}$ (at 95% *RH*) is shown in Figure 7. When the paper was coated with EVOH, $\gamma$ is affected to a greater degree by aluminum thickness. When the aluminum thickness was approximately 30–40 nm on EVOH-coated surfaces, $\gamma_{max}$ did not decrease any further. For practical applications, this means that the maximum resistance against hygroexpansion was reached at this thickness;

7.  Accordingly, the crack onset strain (COS) increased with aluminum thickness and decreasing substrate roughness;

8.  Although the hygroexpansion was higher in the presence of EVOH than in its absence, $\gamma_{max}$ on EVOH coated paper was only a little higher. The increase in hygroexpansion due to the EVOH coating was, therefore, not a major hindrance to the production of flexible and closed aluminum coatings.
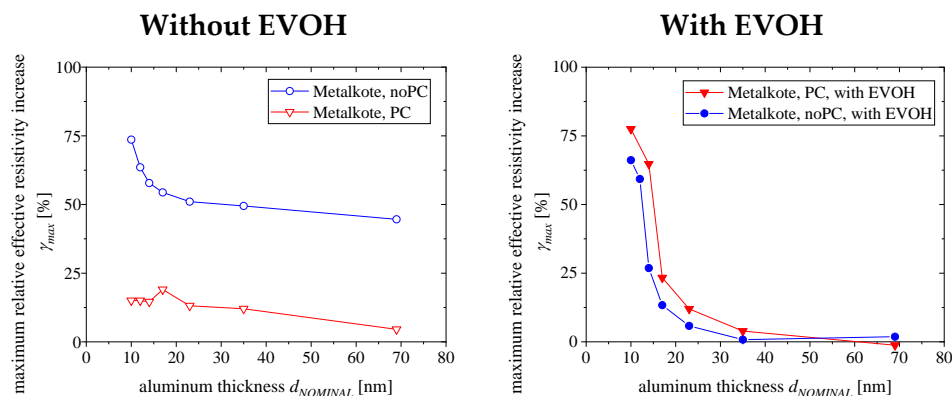


**Figure 7.** When the Metalkote paper was coated with EVOH, the maximum relative effective resistivity increase $\gamma_{max}$ was much more dependent on aluminum thickness. PC/noPC = paper surface with/without pigment coating. EVOH = ethylene vinyl alcohol lacquer.

## 3.4. Effect of Drying Contraction on Electrical Resistivity

Inorganic brittle coatings can recover a part of their characteristic properties, such as conductivity after relaxation, when the applied strain or hygroexpansion, respectively, is removed [29]. In order to determine whether aluminum on paper behaves in a similar manner, the electrical resistivity was compared before and after humidification at 95% *RH*. Before and after humidification, the relative humidity was set to 50% (Figure 8).
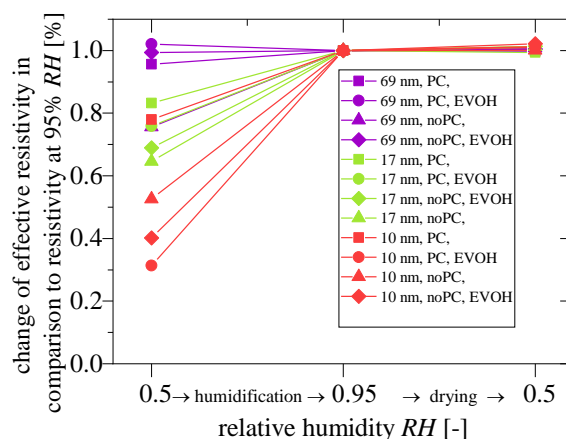
**Figure 8.** After humidification and subsequent drying, the differently coated Metalkote paper samples did not regain their initial resistivity values. PC/noPC = paper surface with/without pigment coating. EVOH = ethylene vinyl alcohol co-polymer lacquer coating as basis for aluminum coating.

The resistivity values were compared by assigning a reference value (=1) at 95% *RH*. We found that the resistivity after drying did not recover its original value, regardless of the substrate roughness, polymer coating or aluminum thickness. We, therefore, anticipate that the gas barrier performance would not be regained once the aluminum has cracked due to moisture uptake and hygroexpansion.

## 4. Conclusions

In this study, we showed that lacquer coating weights were higher when the lacquer was applied on paper surfaces, which were not pigment coated. This probably reflected the porous surface of the paper and its microchannels, which let the lacquer flow into and fill up pores and microchannels. This promoted hygroexpansion, because the lacquer occupied the space that otherwise could be filled by expanding fibers. Alternatively, hygroexpansion could be avoided by using wet-strength paper, which is hydrophobized and where fibers are cross-linked.

When pure paper or paper covered with lacquer was coated with aluminum via PVD, the effective resistivity increased with the roughness, hygroexpansion and the thinness of the aluminum layer. The crack onset point (COS) decreased with increasing substrate roughness and aluminum thinness. The relative effective resistivity increase only depended on aluminum thickness when the substrate was smooth and free of pores. Regardless of the substrate, we found that an aluminum thickness of >35 nm did not further improve the mechanical stability of the aluminum coatings under hygroexpansion-induced tension. For practical applications, this means that ~35 nm is the aluminum thickness that achieves the greatest avoidance of hygroexpansion and roughness induced defects while using the minimum amount of coating material. However, cracked aluminum barrier coatings did not regain their initial resistivity during re-contraction. This means it is critical to avoid hygroexpansion-induced defects.

## References

1.  Lindner, M.; Heider, J.; Reinelt, M.; Langowski, H.-C. Hygroexpansion and surface roughness cause defects and increase the electrical resistivity of physical vapor deposited aluminum coatings on paper. *Coatings* **2019**, *9*, 33. [CrossRef]
2.  Lindner, M.; Schmid, M. Thickness measurement methods for physical vapor deposited Aluminum Coatings in Packaging Applications: A Review. *Coatings* **2017**, *7*, 9. [CrossRef]
3.  Kijima, T.; Yamakawa, I. Effect of beating condition on shrinkage during drying. *Jpn. Tappi J.* **1978**, *32*, 722–727. [CrossRef]
4.  Salmén, L.; Boman, R.; Fellers, C.; Htun, M. The implications of fiber and sheet structure for the hygroexpansivity of paper [curl, shrinkage, beating, fines]. *Nord. Pulp Pap. Res. J. (Sweden)* **1987**, *4*, 127. [CrossRef]
5.  Antonsson, S.; Mäkelä, P.; Fellers, C.; Lindström, M.E. Comparison of the physical properties between hardwood and softwood pulps. *Nord. Pulp Pap. Res. J.* **2009**, *24*, 409–414. [CrossRef]
6.  Mendes, A.H.T.; Kim, H.Y.; Ferreira, P.J.T.; Park, S.W. The importance of the measurement of paper differential CD shrinkage. *O PAPEL* **2012**, *73*, 45–50.
7.  Fahey, D.J.; Chilson, W. Mechanical treatments for improving dimensional stability of paper. *Rev. Process. Non-Refereed (Other)* **1963**, *46*, 393–399.
8.  Sampson, W.W.; Yamamoto, J. The drying shrinkage of cellulosic fibres and isotropic paper sheets. *J. Mater. Sci.* **2011**, *46*, 541–547. [CrossRef]
9.  Lif, J.O. Hygro-viscoelastic stress analysis in paper web offset printing. *Finite Elem. Anal. Des.* **2006**, *42*, 341–366. [CrossRef]
10. Alfthan, J. The Effect of Humidity Cycle Amplitude on Accelerated Tensile Creep of Paper. *Mech. Time-Depend. Mater.* **2004**, *8*, 289–302. [CrossRef]
11. Dickerman, G.K.; Savage, R.L. Method of Making Printable Coated Paper. U.S. Patent 2949382, 28 February 1960.
12. DeMatte, M.L.; Kelly, S.T. Coated Paper for Inkjet Printing. U.S. Patent 5985424A, 16 November 1999.
13. Kuroyama, Y.; Ohmura, T.; Yamazaki, Y.; Nanri, Y. Cast-Coated Paper for Ink Jet Recording and Production Method Thereof. U.S. Patent 5755929, 26 May 1998.
14. Paunonen, S. Influence of Moisture on the Performance of Polyethylene Coated Solid Fiberboard and Boxes. Ph.D. Thesis, Norwegian University of Science and Technology, Trondheim, Noway, October 2010.
15. *DIN EN ISO 3274:1998-04. Geometrical Product Specifications (GPS)—Surface Texture: Profile method—Nominal Characteristics of Contact (stylus) Instruments (ISO 3274:1996)*, German version EN ISO 3274:1997; Beuth: Berlin, Germany, 1998.
16. *DIN EN ISO 4288:1998-04. Geometrical Product Specifications (GPS)—Surface Texture: Profile method—Rules and Procedures for the Assessment of Surface Texture (ISO 4288:1996)*, German version EN ISO 4288:1997; Beuth: Berlin, Germany, 1998.
17. Zhang, Z.; Britt, I.J.; Tung, M.A. Permeation of oxygen and water vapor through EVOH films as influenced by relative humidity. *J. Appl. Polym. Sci.* **2001**, *82*, 1866–1872. [CrossRef]
18. Johansson, C.; Clegg, F. Hydrophobically modified poly (vinyl alcohol) and bentonite nanocomposites thereof: Barrier, mechanical, and aesthetic properties. *J. Appl. Polym. Sci.* **2015**, *132*, 41737. [CrossRef]
19. Lindner, M.; Höflsauer, F.; Heider, J.; Reinelt, M.; Langowski, H.-C. Comparison of thickness determination methods for physical-vapor-deposited aluminum coatings in packaging applications. *Thin Solid Film.* **2018**, *666*, 6–14. [CrossRef]
20. Kaden, H. *Wirbelströme und Schirmung in der Nachrichtentechnik*; Springer: Heidelberg, Germany, 2007.
21. Küpfmüller, K.; Mathis, W.; Reibiger, A. *Theoretische Elektrotechnik: Eine Einführung*; Springer: Heidelberg, Germany, 2006.
22. Lu, N.; Wang, X.; Suo, Z.; Vlassak, J. Metal films on polymer substrates stretched beyond 50%. *Appl. Phys. Lett.* **2007**, *91*, 221909. [CrossRef]
23. Sorg, H. *Praxis der Rauheitsmessung und Oberflächenbeurteilung*; Hanser: Munich, Germany, 1995.
24. Ridgway, C.J.; Gane, P.A. Bulk density measurement and coating porosity calculation for coated paper samples. *Nord. Pulp Pap. Res. J.* **2003**, *18*, 24–31. [CrossRef]

25.  Oliver, J.; Agbezuge, L.; Woodcock, K. A diffusion approach for modelling penetration of aqueous liquids into paper. *Colloids Surf. A Physicochem. Eng. Asp.* **1994**, *89*, 213–226. [CrossRef]

26.  Roberts, R.J. Liquid Penetration into Paper. Ph.D. Thesis, Australian National University September, Canberra, Australia, September 2010.

27.  Hyväluoma, J.; Raiskinmäki, P.; Jäsberg, A.; Koponen, A.; Kataja, M.; Timonen, J. Simulation of liquid penetration in paper. *Phys. Rev. E* **2006**, *73*, 036705. [CrossRef] [PubMed]

28.  Viguie, J.; Dumont, P.J.J.; Mauret, E.; du Roscoat, S.R.; Vacher, P.; Desloges, I.; Bloch, J.F. Analysis of the hygroexpansion of a lignocellulosic fibrous material by digital correlation of images obtained by X-ray synchrotron microtomography: application to a folding box board. *J. Mater. Sci.* **2011**, *46*, 4756–4769. [CrossRef]

29.  Polywka, A.; Stegers, L.; Krauledat, O.; Riedl, T.; Jakob, T.; Görrn, P. Controlled Mechanical Cracking of Metal Films Deposited on Polydimethylsiloxane (PDMS). *Nanomaterials* **2016**, *6*, 168. [CrossRef] [PubMed]